The Familial Mediterranean Fever Protein Interacts and Colocalizes with a Putative Golgi Transporter (44511)

XIAOGUANG CHEN,* YELENA BYKHOVSKAYA,* NICOLA TIDOW,† MELANIE HAMON,* ZOYA BERCOVITZ,* OLGA SPIRINA,* AND NATHAN FISCHEL-GHODSIAN*,[1]

Ahmanson Department of Pediatrics, Steven Spielberg Pediatric Research Center, Medical Genetics Birth Defects Center, and †Department of Medicine, Cedars-Sinai Medical Center and UCLA School of Medicine, Los Angeles, California 90048

Abstract. **The biological function of pyrin, the protein mutated in Familial Mediterranean Fever (FMF), has not been elucidated. Based on sequence homology, a transcription factor activity was proposed for this neutrophil-specific protein. In a yeast two-hybrid assay, neither transcription activation activity nor any self interaction was detected for pyrin. Screening of an expression cDNA library of peripheral blood leukocytes using as bait the carboxyl portion of pyrin (amino acids 557–781), which contains most of the FMF mutations, led to the identification of P/M-IP1 (pyrin/marenostrin interacting protein 1). A splice variant of P/M-IP1, GTC-90, had previously been described as a component of the 13S hetero-oligomeric protein complex that stimulates *in vitro* Golgi transport. We have now shown that P/M-IP1 colocalizes with pyrin in the perinuclear cytoplasm of Cos-7 cells and that the interaction between these two proteins is impaired by FMF causing mutations in pyrin. These data suggest that, at some stage of its functional pathway, pyrin resides in the cytoplasm and might be involved in, or impacted by, cellular protein sorting by the Golgi apparatus. The data also imply that P/M-IP1 may be involved in the abnormal inflammatory response that occurs in patients with FMF.** [P.S.E.B.M. 2000, Vol 224:32–40]

Familial Mediterranean Fever (FMF) is an autosomal recessive genetic disease clinically characterized by periodic attacks of fever and sterile inflammation in the joints, peritoneum, and pleura (1, 2). No characteristic findings can be found in patients experiencing an attack or being in remission other than a polymorphonuclear leukocyte infiltration of the anatomic cavities defined by the serosal membranes and an increase in acute phase reactants and erythrocyte sedimentation rate. It was hoped that the identification of the gene responsible for FMF would lead to a better understanding of the dysregulated inflammatory response in this disease. Unfortunately, positional cloning of *MEFV*, the gene responsible for FMF, did not lead to any immediate insight into the inflammatory pathway involved in FMF. *MEFV* encodes a transcript of ≈ 3.7 kilobases that is expressed mainly in peripheral blood leukocytes, and codes for a protein called pyrin or marenostrin (3, 4). Protein sequence analysis revealed five different motifs/conserved domains: i) a bZIP basic domain (amino acids 266–270); ii) a B-Box zinc finger domain (amino acids 375–407); iii) a coiled-coil domain (amino acids 408–594); iv) a B30.2 domain (amino acids 598–774); and v) two nuclear localization signals (amino acids 157–163 and 420–437). By homology the bZIP basic domain and the B-Box zinc finger were speculated to confer DNA binding and transcription modulation activity; the coiled-coil domain was proposed to mediate protein-protein interaction including homo-dimerization; and the nuclear localization signals were postulated to localize the protein to the cell nucleus. Based on such computational studies, pyrin was proposed to be a nuclear transcription factor that regulates inflammation (3).

This study was supported by a Cedars-Sinai Research Institute Academic Enrichment fund, and N. Tidow is recipient of a fellowship from the Deutsche Forschungsgemeinschaft.

[1]To whom requests for reprints should be addressed at Department of Pediatrics, Cedars-Sinai Medical Center, 8700 Beverly Blvd., Los Angeles, CA 90048. E-mail: nfischel@xchg.peds.csmc.edu

Received August 6, 1999. [P.S.E.B.M. 2000, Vol 224]
Accepted January 11, 2000.

0037-9727/00/2241-0032$15.00/0

The cloning of the *FMF* gene does allow experimental approaches to understand the biological function of its protein, pyrin. The spectrum of pyrin mutations has been established in FMF patients of different ethnic backgrounds, allowing the establishment of correlations between structural integrity of the protein and its function, and specific phenotypes versus individual disease-causing mutations (5–10). A total of 14 disease-causing mutations have been described so far. Nine of them, all in exon 10 of *MEFV*, disrupt the primary structure of the B30.2 domain. Another two mutations, affecting the coiled-coil domain, are found in exon 5, whereas the remaining three mutations in exon 2 have no apparent impact on the primary structure of any of the structural motifs/conserved domains predicted in pyrin (5–7). A strong association between amyloidosis and the Met694Val mutation, one of those mutations that disrupts the B30.2 domain, has been described although the mechanism of how such a mutation predisposes to amyloidosis remains unknown (8–10). The tissue expression of pyrin has also been carefully documented. Consistent with our initial report (3), pyrin is expressed preferentially in granulocytes and myeloid bone marrow precursors, and its expression is enhanced in HL-60 cells undergoing stimulated granulocytic differentiation (5, 11).

In the current study, we tried to approach the biological function of pyrin through the use of the yeast two-hybrid assays (12). The proposed transcriptional factor activity of pyrin and its ability to form homo-dimers were tested. Moreover, we looked for proteins that could interact with the pyrin peptide having the highest mutation load. We provide evidence here that this granulocyte-specific protein colocalizes and interacts with an isoform of a component of the 13S hetero-oligomeric protein complex that has been shown *in vitro* to stimulate Golgi transport (13).

Materials and Methods

Recombinant Plasmids. Yeast two-hybrid system 2 vectors pAS2-1 and pACT2 (Clontech, Palo Alto, CA) were used to construct *GAL* 4 BD and *GAL* 4 AD hybrids. An *Nco*I restriction fragment encompassing nucleotides 41–2601 and harboring the complete open reading frame of *MEFV*, was inserted into the *Nco*I site of either pAS2-1 or pACT2, respectively, to construct full-length pyrin/*GAL* 4 BD and full-length pyrin/*GAL* 4 AD hybrids. Pyrin (amino acids 1–305)/*GAL* 4 BD, pyrin (amino acids 299–563)/*GAL* 4 BD, and pyrin (amino acids 557–781)/*GAL* 4 BD hybrids were constructed using the following cloning strategy. Nucleotides encoding the peptide of interest were amplified using one of three sets of PCR primers:

fmfytf1 5′ > gactttctgaattcatggctaagacccctagtga < 3′

fmfytr1 5′ > acttcaaggtcgaccttccggtgaccgaatgtt < 3′

fmfytf2 5′ > gactttctgaattcgaacattcggtcaccggaag < 3′

fmfytr2 5′ > acttcaaggtcgaccttctggtggaggagttgga < 3′

fmfytf3 5′ > gactttctgaattcatccaactcctccaccagaa < 3′

fmfytr3 5′ > acttcaaggtcgacagtgttgggcattcagtcag < 3′

The *EcoR* I and *Sal* I recognition sequences attached (underlined sequences in each primer) allowed directional cloning of the amplified DNA fragments into pAS2-1 at its *EcoR* I/*Sal* I sites. A recombinant plasmid containing wild-type *MEFV* (provided by Dr. Daniel L. Kastner) served as PCR template. For preparation of the mutant pyrin (amino acids 557–781)/*GAL* 4 BD hybrid, cDNA to mRNA of lymphoblastoid cell lines of two patients, one homozygous for the Met694Val mutation and the other homozygous for the Val726Ala mutation, was employed. The study was approved by the Human Subject Committee at the Cedars-Sinai Medical Center, and informed consent was obtained. The ability of each recombinant plasmid to encode the intended peptide was confirmed by DNA sequencing. Testing of transcription activation activity employed all of the pyrin-related *GAL* 4 BD hybrids constructed, whereas only hybrids containing full-length pyrin (full-length pyrin/*GAL* 4 BD and full-length pyrin/*GAL* 4 AD) were assessed for self-interaction. Yeast two-hybrid screen of candidate interacting proteins used the wild-type pyrin (amino acids 557–781)/*GAL* 4 BD hybrid.

Yeast Transformation and Two-Hybrid Screen. Transformation and/or co-transformation of Y187 (*MATa, trp1, leu2::lacZ*) or CG1945 (*MATa, trp1, leu2, cyh^{r}2::HIS3, lacZ*) yeast cells, together with assay for β-galactosidase, was performed as described (14, 15). p53/*GAL* 4 BD (pVA3, Clontech), T-antigen/*GAL* 4 AD (pTD1, Clontech), human lamin C/*GAL* 4 BD (pLAM5′, Clontech), and wild-type *GAL* 4 (pCL1, Clontech) were used as positive or negative controls wherever indicated. The Matchmaker Two-Hybrid System 2 Kit (Clontech protocol PT3061-1) was used to screen a Matchmaker cDNA library of peripheral blood leukocytes (Clontech HL4014AB) according to the manufacturer's protocols; the library was in pGAD10. Screening was performed in CG1945 yeast cells into which pyrin (amino acids 557–781)/*GAL* 4 BD hybrid and target protein/*GAL* 4 AD hybrids had been introduced simultaneously by co-transformation (14). A total of two million primary transformants were selected on the Leu$^-$, Trp$^-$, and His$^-$ plates in the presence of 5 m*M* 3-amino-triazole (3-AT) (Sigma, St. Louis, MO) that suppresses background expression of the *HIS3* gene in CG1945. Colonies were picked and restreaked on the same selection plates before being tested for β-galactosidase activity in a colony-lift assay. Recombinant pGAD10 plasmids were segregated and rescued by manipulations involving first growing the yeast colonies of interest in Leu$^-$ medium, then recovering plasmid DNA from the yeasts, and finally using the resultant plasmid DNA to transform *E. coli* strain HB101. From 67 yeast colonies of interest, 46 recombinant pGAD10 plasmids were recovered. The plasmids were partially sequenced using a dsDNA Cycle Sequencing System (GIBCOBRL, Grand Island, NY) and primers on the

pGAD10 vector (Clontech). Clones with identical end sequences were sorted into groups. Clones from one of the three groups had a cDNA insert of 2.4 kilobases. Analysis of DNA sequence by BLAST (16) used the NCBI BLAST search launcher on the World Wide Web (http://www.ncbi.nlm.nih.gov/BLAST).

Localization of Pyrin/Marenostrin Interacting Protein 1 (P/M-IP1) and Pyrin with Fluorescent Proteins. The fluorescent protein vectors pECFP and pEYFP (Clontech), encoding a cyan and a yellow fluorescent protein, respectively, were used for localization of P/M-IP1 and pyrin in the Cos-7 cells. A cDNA fragment encoding amino acids 1–775 of pyrin was amplified by PCR with primers that carry *Sal* I recognition sequences at their 5′ ends. After *Sal* I digestion, the amplified DNA fragment was cloned into pECFP at the *Sal* I site, and clones encoding a fusion protein with pyrin in its N-terminal portion and ECFP in its C-terminal portion were selected by restriction mapping and DNA sequencing. Construction of the recombinant plasmid encoding the EYFP-P/M-IP1 fusion protein followed a similar scheme by inserting a PCR-amplified *Sal* I–tailed DNA fragment encoding amino acids 1–721 of P/M-IP1 into the pEYFP vector at its *Sal* I site. Cos-7 cells, obtained from the ATCC (American Type Culture Collection), were maintained at 37°C in a humidified atomosphere with 5% carbon dioxide in D-MEM medium supplemented with 10% fetal bovine serum (GIBCOBRL). Cell transfection by SuperFect (QIAGEN, Valencia, CA) was done according to the manufacturer's protocols. For transfection involving a single plasmid, 8×10^5 cells and 5 μg of plasmid DNA were used. Co-transfection with plasmids encoding pyrin/ECFP and P/M-IP1/EYFP was done similarly, except that the amount of DNA used for each plasmid was 2.5 μg instead of 5 μg. Transfectants were grown for 24 hr on coverslides before being fixed in 3.7% paraformaldehyde in PBS for 30 min and analyzed by fluorescence microscopy using XF104 or XF114 filters (Omega).

β-Galactosidase Liquid Assay. Transformation of Y187 yeast cells and semiquantitative determination of β-galactosidase activity were done as described (15). Units of β-galactosidase (β-gal) activity were defined by the formula, $1000 \times OD_{420}/(t \times V \times OD_{600})$, where OD_{420} is from the *o*-nitrophenyl β-D-galactosidase/hydrolysis assay; *t*, time of incubation in minutes; *V*, volume of yeast culture from which the assayed extract sample was prepared; and OD_{600}, absorbance at 600 nm of 1 ml of the yeast culture. β-gal activities shown in Table I are the mean and standard deviations from three independent yeast transformants from each of two independent experiments.

Northern Blotting and RT-PCR. Multiple Tissue Northern Blots (Clontech) for adult human tissues were hybridized with the 2.4-kb cDNA of P/M-IP1 recovered from the yeast two-hybrid screening. Hybridization was done in ExpressHyb Hybridization Solution (Clontech) according to the manufacturer's instructions. Auto-radiography was at –80°C overnight with intensifying screens. Expression of P/M-IP1 in normal adult human tissues was assessed by RT-PCR using cDNA from human testis, spleen, prostate, ovary, muscle, lung, kidney, heart, small intestine, brain, and peripheral blood leukocytes (OriGene Technologies, Inc. Rockville, MD). Primers used were: 5′ > gtttcattgccagagttat < 3′ and 5′ > aatttaccagcttaatcttg < 3′ with an annealing temperature of 55°C.

Results

Pyrin Lacks Transcription Activation Activity and Does Not Form Homo-Dimers in the Yeast Cells. As a prerequisite to use pyrin as bait in a two-hybrid screen of an expression cDNA library of peripheral blood leukocytes, it had to be ruled out that pyrin has intrinsic transcription factor activity. This is especially important because, as mentioned earlier, pyrin was proposed to be a transcriptional regulator (3). To test this, different peptides of pyrin were fused in frame with the DNA binding domain (BD) of *GAL* 4, and the fusion constructs were tested for transcription activation activity in the yeast strain Y187, a yeast cell having, as its genomic constituent, two copies of the *lacZ* gene whose expressions are controlled by *GAL* 4. The native transcription factor *GAL* 4 contained in the plasmid pCL1 (Clontech) was used as a positive control. No expression of *lacZ* was detected for any of the pyrin/*GAL* 4 BD fusion proteins tested, suggesting a lack of transcription activation activity. What needs to be emphasized, however, is the fact that transcription downregulation goes undetected in such an assay system.

Amino acids 408–594 of pyrin were predicted to assume a secondary structure of an α-helix or a coiled-coil domain capable of mediating protein-protein interactions, including formation of homo-dimers (3, 5). As a direct test to this, a two-hybrid assay was performed. The hybrids were constructed in such a way that one expresses a full-length pyrin/*GAL* 4 BD fusion protein, and the other, a full-length

Table I. Interaction Between P/M-IP1 and Wild-Type or Mutant Pyrin

	GAL 4 BD hybrids[a]			
GAL 4 AD hybrid[c]	Wild-type pyrin	Pyrin/Met694Val	Pyrin/Val726Ala	pAS2-1[b]
	1.20 (0.01)[d]	0.37 (0.02)	0.34 (0.03)	0.18 (0.01)

[a] The *GAL* 4 BD hybrids used are recombinant plasmids of pAS2-1 that encode pyrin (amino acids 557–781)/*GAL* 4 BD fusion proteins.
[b] The control plasmid encoding GAL 4 BD only, used here as a negative control.
[c] The *GAL* 4 AD hybrid here refers to the pGAD10 recombinant plasmid encoding P/M-IP1/*GAL* 4 AD fusion protein.
[d] The mean β-galactosidase activity with standard deviations (SD).

pyrin/*GAL* 4 transcription activation domain (*GAL* 4 AD) fusion protein. Any self-interaction or dimerization of pyrin will lead to the reconstitution of a functional *GAL* 4 protein that in turn activates reporter constructs responsive to *GAL* 4, such as the *lacZ* construct in the yeast strain Y187. The hybrids were introduced into the yeast strain Y187 by co-transformation, and the co-transformants were assessed for presence of β-galactosidase activity by the β-galactosidase colony lift assay. No activation of *lacZ* expression was revealed, suggesting that pyrin does not interact with itself to form homo-dimers in the yeast.

Pyrin Interacts with P/M-IP1, an Isoform of GTC-90. To identify proteins that interact with pyrin, an expression cDNA library of peripheral blood leukocyte (Clontech) in the pGAD10 vector was screened using a pyrin peptide (amino acids 557–781) as bait in a yeast two-hybrid assay with PEG/LiAc-mediated co-transformation of CG1945 yeast cells (14). An estimated 2×10^6 primary co-transformants were obtained using 1 mg of plasmid DNA for the pyrin (amino acids 557–781)/*GAL 4* BD hybrid and 500 μg of plasmid DNA for the target protein/*GAL 4* AD hybrids. Cells containing candidate pyrin-interacting molecules were identified both by their ability to grow in the absence of leucine, tryptophan, and histidine, and by the presence in them of β-galactosidase activity, which was assessed by colony lift assay. Of 67 yeast colonies that passed this selection, 46 contained recombinant pGAD10 plasmids that, in conjunction with the bait plasmid, consistently and reproducibly induced transcription from the *lacZ* and *His3* reporter constructs in the CG1945 yeast cells and transcription from the *lacZ* reporter construct in the Y187 yeast cells. The 46 plasmids were sorted into three groups according to features of their partial sequences. Two of the groups showed no significant homology to any known human proteins. The last group had a cDNA insert of about 2.4 kb, with a stretch of 30 adenines (A) attached at its 3′ end. Search of the database of expressed sequence tags (dbEST) by BLAST (16) using sequences from the 5′ end of the 2.4-kb cDNA revealed multiple ESTs having identical sequences, whereas no hits were revealed in similar searches when its 3′ end sequence of 252 bp was used. A consensus sequence of 2553 bp, encoding a polypeptide of 733 amino acids with an estimated molecular size of 81 kDa, was assembled for the gene represented by the 2.4-kb cDNA by progressive sequence alignment for homologous ESTs. The amino acids predicted for this gene were exactly the same as those for codons 1–733 of GTC-90, a brain specific component of the recently described 13S hetero-oligomeric protein complex that stimulates *in vitro* Golgi transport (13). However, nucleotides for amino acids 734–839 of GTC-90 were absent in the gene represented by the 2.4-kb cDNA clone. Moreover, its 3′ untranslated region (3′ UTR) differs from that of GTC-90 in sequence, suggesting that the corresponding gene is a truncated isoform of GTC-90. This was confirmed, as described later, by study of its tissue expression and genomic structure. Since this is the first pyrin/marenostrin interacting protein characterized, we called it P/M-IP1.

Pyrin and P/M-IP1 Colocalize to the Perinuclear Cytoplasm of Cos-7 Cells. To test for physiological relevance of this putative interaction, subcellular localization of the interacting proteins was performed. Two expression fusion constructs were prepared and introduced, individually or together, into the mammalian cell line Cos-7 by transfection. In one of the fusion constructs, the open reading frame for pyrin was fused in frame and 5′ of that for the enhanced green fluorescent protein variant, cyan fluorescent protein (ECFP). In the other construct, the open reading frame for P/M-IP1 was fused to that for yellow fluorescent protein in a similar manner. The auto-fluorescence generated by the C-terminal portions of each fusion protein allowed determination of its subcellular localization (17). Previous reports concerning the subcellular localization of GTC-90 had suggested a perinuclear localization (13), and preliminary results by us had indicated a similar distribution for pyrin. Review of these results indicated that the distribution of the proteins around the nucleus was not homogeneous, but appeared to be localized more to one side of the nucleus, giving a "capping" appearance (13). Consistent with these observations, asymmetric perinuclear cytoplasmic auto-fluorescence was observed for both pyrin and P/M-IP1 when the fusion construct for each was individually introduced into Cos-7, and transiently expressed (Figs. 1b & 1d). In general, the blue fluorescence of the pyrin fusion protein was more predominant within the cell than the yellow fluorescence of the P/M-IP1 fusion protein. Co-transfection of Cos-7 cells with both fusion constructs demonstrated, in all the cells with both blue and yellow fluorescence, that the blotches of yellow fluorescence were within the blotches of blue fluorescence (Fig. 1e). These experiments strongly suggest that pyrin and P/M-IP1 colocalize.

Disease-Causing Mutations in Pyrin Decrease its Interaction with P/M-IP1. The next step was to examine whether the observed interaction can be affected by FMF causing mutations in pyrin. Demonstration of such an effect would not only support the physical interaction of these two proteins, but would also indicate that P/M-IP1 is likely to be involved in a physiologically relevant part of the inflammatory pathway in FMF. Nucleotides 1711–2400 of *MEFV*, encoding amino acids 557–781 of pyrin, were amplified from cDNA of lymphoblastoid cell lines derived from two FMF patients. One of the patients was a homozygote for the Met694Val mutation, and the other, a homozygote for the Val726Ala mutation. The primers, PCR conditions, and cloning strategies employed were identical to those used for the preparation of the normal pyrin bait used in the yeast two-hybrid screening. However, extended PCR cycles were employed due to the very low expression of pyrin in lymphoblastoid cell lines. The nucleotide sequences of the bait prepared, in particular the presence of the expected mutations, were confirmed by sequencing.

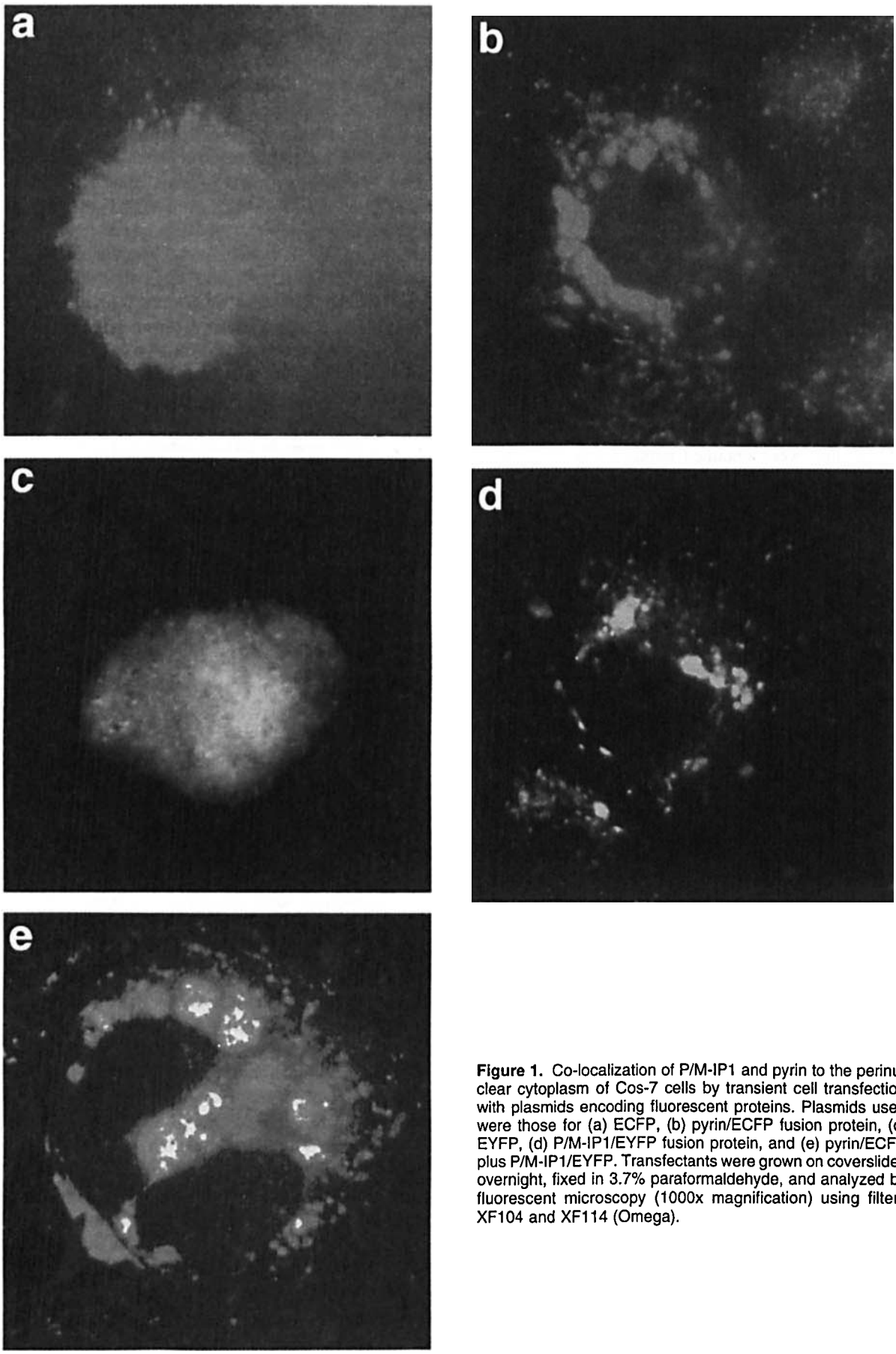

Figure 1. Co-localization of P/M-IP1 and pyrin to the perinuclear cytoplasm of Cos-7 cells by transient cell transfection with plasmids encoding fluorescent proteins. Plasmids used were those for (a) ECFP, (b) pyrin/ECFP fusion protein, (c) EYFP, (d) P/M-IP1/EYFP fusion protein, and (e) pyrin/ECFP plus P/M-IP1/EYFP. Transfectants were grown on coverslides overnight, fixed in 3.7% paraformaldehyde, and analyzed by fluorescent microscopy (1000x magnification) using filters XF104 and XF114 (Omega).

To compare the strength of interaction between P/M-IP1//wild-type pyrin and P/M-IP1//mutant pyrin, co-transformation of the yeast strain Y187 and semiquantitative β-galactosidase liquid assays were performed. Co-transformation of the yeast employed a pGAD10 recombinant plasmid encoding P/M-IP1 plus a pAS2–1 recombinant plasmid encoding either wild-type pyrin or pyrin carrying one of the two disease-causing mutations, Met694Val or Val726Ala. Three transformants from each co-transformation reaction were picked, and the magnitude of their β-galactosidase activities, determined by β-galactosidase liquid assays. Each co-transformation reaction was then repeated in an independent experiment. Table I summarizes the results from both experiments. An over 75% decrease in the strength of interaction was observed when pyrin contained either of the two FMF-causing mutations, suggesting that the interaction between pyrin and P/M-IP1 might be biologically important.

P/M-IP1 Is Widely Expressed and Differentially Spliced. To further characterize P/M-IP1, we studied its tissue expression and genomic structure. Amplification by PCR of nucleotides 1920–2415 of P/M-IP1, which spans 84 of its N-terminal codons and most of its 3′ UTR, from cDNA of different human tissues revealed widespread tissue expression of P/M-IP1 in all of the tissues tested except brain and liver (Fig. 2A), giving further support that this is an isoform different from GTC-90 since the latter is known to be expressed in the brain (13). As demonstrated in Figure 2C, hybridization bands of different sizes were revealed when the 2.4-kb cDNA of P/M-IP1 was hybridized with mRNA from a panel of eight different adult human tissues. Three major transcripts of ≈ 2.7 kb, 3.8 kb, and 5.2 kb were detected in all eight different tissues tested, and an additional low-level 2.5-kb transcript was seen in peripheral blood leukocytes and testis.

To understand the mechanism(s) underlying the differential splicing of P/M-IP1 and its related isoforms, we determined their genomic structures. This was greatly facilitated by an ongoing genomic sequencing project for human chromosome 7 (18). The entire cDNA sequence of P/M-IP1, together with that of its brain isoform GTC-90, was found by BLAST search of the nonredundant database to be encoded by 485 kb of genomic DNA from the 7q22–31 chromosomal region encompassed by two BAC clones (RG020D02, and RG363E19) and a PAC clone (DJ067311) (19–21). Nineteen exons were identified for P/M-IP1, and three more were recognized for GTC-90, making the total number of exons for GTC-90 22 (Fig. 3). The exons varied greatly in size from 55 base pairs (exon 4) to 1073 base pairs (exon 22). Similar dramatic size differences were observed for the intervening introns, with intron 4 being the smallest (97 base-pairs), and intron 6, the largest (114 kilobases), having a putative G protein–coupled receptor encoded on the strand opposite of that for P/M-IP1 or GTC-90 (20). Interestingly, the genomic region for P/M-IP1 coincides with the chromosomal region frequently deleted in hematologic diseases, such as myeloid leukemia and abnormality in neutrophil chemotaxis (22, 23). However, RT-PCR studies and analyses of P/M-IP1 cDNA sequences revealed no abnormalities in three leukemia cell lines (HL-60, ML-1, and U937) other than a missense change that switches codon 330 of P/M-IP1 from leucine (CTC) to phenylalanine (TTC). The same change was found in the lymphoblastoid cell line cDNAs of several FMF patients, suggesting that this is more likely a polymorphism rather than a disease-causing mutation.

Consistent with multiple messages observed on Northern studies, differential splicing was revealed for this gene when cDNA sequences for P/M-IP1, GTC-90, and their homologous ESTs were compared and aligned with their corresponding genomic sequences. As illustrated in Figure 3, differential splicing involving exon 19 gave rise to transcripts that were close in size to the 2.7-kb and 3.8-kb mRNA detected on Northern blots. Differential splicing involving exons other than exon 19 was also found. They included a read-through into the intron at the 3′ end of exon 5; an insertion of an extra exon between exons 7 and 8, and again between exons 16 and 17; and a skip of exon 16 (Fig. 3, hatched boxes and dotted lines). Interestingly, some of these latter splice events, such as the one that skipped exon 16, led to premature termination of translation. The biological significance of these latter splice events is unknown since they are observed with almost equal frequencies in both normal and cancerous tissues. Given the large genomic size of this gene, some of the differential splicing observed may represent immature splicing that leads to low-level transcripts of different sizes observed on Northern blots.

Discussion

In the current study, we tested the proposed transcription factor activity of pyrin and its ability to form homodimers through the use of the yeast two-hybrid assays. Failure of the various pyrin/*GAL* 4 BD constructs to activate expression from the *GAL* 4–responsive *lacZ* reporter in the Y187 yeast cells argues against transcription activation activity in pyrin. Similarly, lack of expression from the *lacZ* locus in the Y187 yeast cells co-transformed with both full-length pyrin/*GAL* 4 AD and full-length pyrin/*GAL* 4 BD hybrids does not support the previous proposition based on sequence analysis that pyrin might form homo-dimers *via* the self-interaction of its coiled-coil domain (5). However, cautions must be exercised not to over-interpret the significance of these observations due to the following concerns: First, the reconstitution of functional *GAL* 4 protein used in this study is sensitive only to the detection of transcription activation activity. It does not allow assessment of transcription repression, which can be a problem for pyrin since its associated clinical phenotype favors more of a transcription repressor than of an activator. Secondly, the yeast two-hybrid assay is a heterologous system that differs from the mammalian environment in which pyrin resides. Post-translational modifications indispensable to its secondary

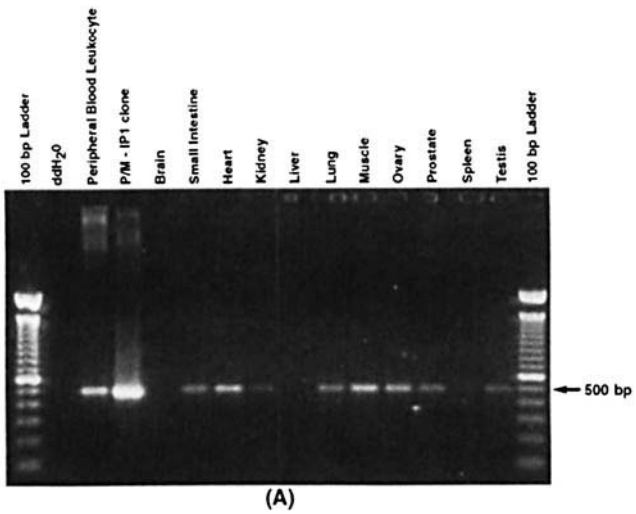

(A)

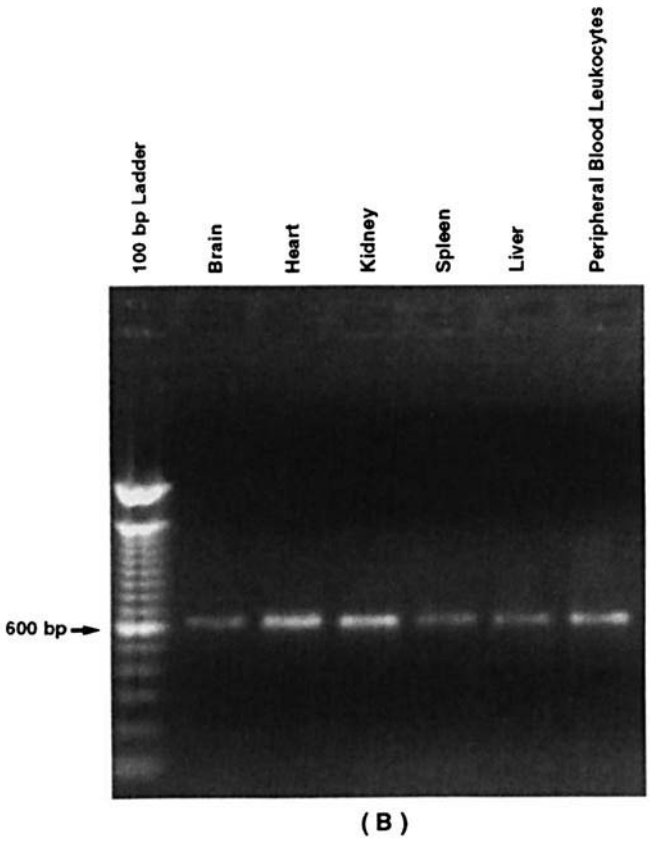

(B)

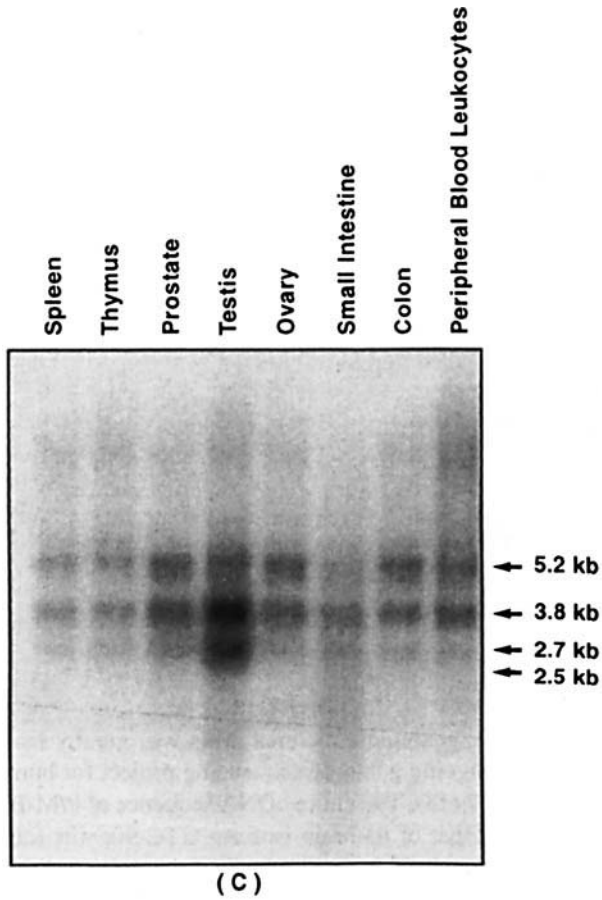

(C)

Figure 2. Expression of P/M-IP1 in normal adult human tissues. (A) Nucleotides 1920–2415 of P/M-IP1 were amplified by PCR from cDNA of human testis, spleen, prostate, ovary, muscle, lung, kidney, heart, small intestine, brain, and peripheral blood leukocytes. The 2.4-kb cDNA of P/M-IP1 was used as a positive control. PCR products were resolved on a 1% agarose gel and visualized by ethidium bromide staining. A PCR product of expected size (495 bp) was detected in all of the tissues tested except in brain and liver. PCR amplification of α-actin was performed to ensure the quality of the cDNA template, especially those that give negative amplification for P/M-IP1 (B). (C) mRNA from multiple human tissues was hybridized with the 2.4-kb cDNA of P/M-IP1. Three major transcripts of 2.7, 3.8, and 5.2 kb were detected in eight different adult human tissues. A minor transcript of 2.5 kb can be seen in peripheral blood leukocytes and testis.

structure and function may not be available from the yeasts (24, 25).

It is interesting to note that one of the three pyrin-interacting proteins recovered by our yeast two-hybrid screen of an expression cDNA library of peripheral blood leukocytes appears to be cytoplasmic based on our data presented here, and our recent data strongly suggest a cytoplasmic location for the other two proteins as well. Subcellular co-localization of P/M-IP1 with pyrin to the perinuclear cytoplasm of Cos-7 cells and demonstration that the strength of interaction between P/M-IP1 and pyrin decreases significantly when the latter contains either of two frequent FMF-causing mutations impart biological importance to their interaction, and link pyrin, a protein of unknown function, to a particular cytoplasmic process, most likely vesicular transport by the Golgi apparatus.

As has been described, P/M-IP1, the first pyrin-interacting protein characterized in detail, is a truncated isoform of GTC-90, one of the five components of the recently described 13S hetero-oligomeric Golgi transport complex (GTC). *In vitro* studies done by Walter *et al.* demonstrated that GTC-90 stimulates vesicular transport by the Golgi apparatus, and such an activity is abolished by anti-GTC-90 antibodies (13). P/M-IP1 differs from GTC-90 only by a lack of a C-terminal peptide of 106 amino acids present in the latter, making it likely that P/M-IP1 serves a

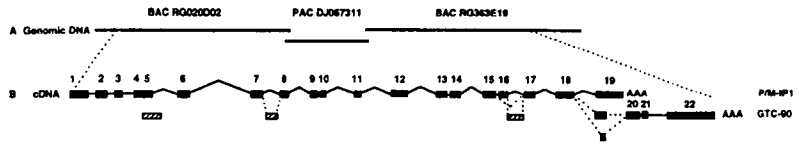

Figure 3. Schematic representation of the genomic structure and differential splicing of P/M-IP1 and its splice variants. (A) Two BAC clones (RG020D02, and RG363E19) and one PAC clone (DJ067311) encoding the various exons of P/M-IP1 and its differentially spliced variants are depicted as solid lines. Black boxes denote exons, which are numbered from 1 through 22. Introns are depicted as solid thin lines connecting exons. Dotted lines between exons represent differential splicing. Hatched boxes are additional/variant exonic sequences derived from differential splice events involving exons other than exon 19. Polyadenine tracks were represented by "AAA" at the end of each transcript. (B) The sizes of the transcripts without their 3′ polyadenine tracks are 2553 bp for P/M-IP1 and 3581 bp for GTC-90.

similar biologic function as does GTC-90, although this needs to be confirmed by direct experiments. Given such a possible function of P/M-IP1 and its specific interaction with pyrin, what remains to be elucidated is to what extent such an interaction contributes to the FMF pathology, since so far the only known connection between the Golgi apparatus and inflammation is the presence of auto-antibodies against Golgi membrane–associated proteins in patients of autoimmune, inflammatory diseases, such as rheumatoid arthritis, systemic lupus erythematosus, and Sjogren's syndrome (26–28).

Another interesting feature of P/M-IP1 that stimulates further study of its possible role in the FMF pathology is its genomic structure and chromosomal location. This gene spans 485 kb of genomic DNA from the 7q22–31 chromosomal region that is frequently deleted in malignant myeloid diseases and also in a rare disease featuring abnormalities in neutrophil chemotaxis (22, 23). Part of the FMF pathology is excessive neutrophil chemotaxis, and one of the possible functional implications of pyrin as revealed by expression studies is its involvement in the differentiation of myeloid precursor cells (5, 11). By demonstration of structural integrity of P/M-IP1 in three leukemia cell lines (HL-60, ML-1, and U937), our study tentatively excluded this gene as the one responsible for malignant myeloid diseases that have their genetic defect mapped to the 7q22–31 region. However, involvement of P/M-IP1 in abnormal neutrophil chemotaxis remains to be excluded.

In conclusion, using the yeast two-hybrid approach, we tentatively excluded the transcription activation activity of pyrin and its ability to form homo-dimers. An isoform of a component of the 13S hetero-oligomeric Golgi transport complex (GTC-90) was recovered as a putative pyrin interacting protein, and its physiological role is supported by two lines of evidence: First, the physical interaction as measured in the yeast two-hybrid assay is significantly impaired when FMF mutations are present in pyrin; and second, pyrin and P/M-IP1 appear to colocalize in the perinuclear region of the cell. These observations provide experimental evidence in support of pyrin as a cytoplasmic protein possibly involved in cellular protein sorting by the Golgi apparatus. However, it must also be realized that the proposed interaction between pyrin and P/M-IP1 requires additional experimental evidence, in particular to support a physiologically significant role. Such experiments include such experimental approaches as confocal microscopy to demonstrate that the two proteins colocalize, coimmunoprecipitation which despite all its limitations can provide additional support for physical interaction, overexpression and inhibition of both proteins in cellular systems, and studies of both proteins in mouse models of FMF when attempts to generate them are successful. The work presented here represents only the first step in the elucidation of the inflammatory pathway impacted by pyrin.

The authors wish to thank Drs. Z. Shi and X. Chen in Dr. J. Korenberg's laboratory at Cedars-Sinai Medical Center, for their advice on the use of fluorescent proteins and fluorescent microscopy.

1. Heller H, Sohar E, Sherf L. Familial Mediterranean Fever. Arch Intern Med **102**:50–71, 1958.
2. Kastner DL. Intermittent and periodic arthritic syndromes. In: Koopman WJ, Ed. Arthritis and Allied Conditions (13th ed). Baltimore: Williams & Wilkins, pp1279–1306, 1996.
3. The International FMF Consortium. Ancient missense mutations in a new member of the RoRet gene family are likely to cause Familial Mediterranean Fever. Cell **90**:797–807, 1997.
4. The French FMF Consortium. A candidate gene for Familial Mediterranean Fever. Nature Genet **17**:25–31, 1997.
5. Centola M, Aksentijevich I, Kastner DL. The hereditary periodic fever syndromes: Molecular analysis of a new family of inflammatory diseases. Hum Mol Genet **7**:1581–1598, 1998.
6. Bernott A, da Silva C, Petit JL, Cruaud C, Caloustian C, Castet V, Ahmed-Arab M, Dross C, Dupont M, Cattan D, Smaoui N, Dode C, Pecheux C, Nedelac B, Medaxian J, Rozenbaum M, Rosner I, Delpech M, Grateau G, Demaille J, Weissenbach J, Touitou I. Non-founder mutations in the *MEFV* gene establish this gene as the cause of Familial Mediterranean Fever (FMF). Hum Mol Genet **7**:1317–1325, 1998.
7. Chen X, Fischel-Ghodsian N, Cercek A, Hamon M, Ogur G, Lotan R, Danon Y, Shohat M. Assessment of pyrin gene mutations in Turks with Familial Mediterranean Fever. Hum Mutat **11**:456–460, 1998.
8. Shohat M, Magal N, Chen X, Danon Y, Lotan R, Ogur G, Tokguz G, Schlezinger M, Halpern GJ, Schwabe A, Shohat T, Kastner DL, Rotter JI, Fischel-Ghodsian N. Phenotype genotype correlation in Familial Mediterranean Fever: Evidence for an association between Met694Val and amyloidosis. Eur J Hum Genet **7**:287–292, 1999.
9. Pras E, Langevitz P, Livneh A, Zemer D, Migdal A, Padeh S, Lubetzsk A, Aksentijevich I, Centola M, Zaks N, Deng Z, Sood R, Kastner DL, Pras M. Genotype-phenotype correlation in Familial Mediterranean Fever (a preliminary report). In: Sohar E, Gafni J, Pras M, Eds. Familial Mediterranean Fever. Tel Aviv: Freund, pp260–264, 1997.
10. Dewalle M, Domingo C, Rozenbaum M, Ben-Chetrit E, Cattan D, Bernot A, Dross C, Dupont M, Notarnicola C, Levy M, Rosner I, Demaille J, Touitou I. Phenotype-genotype correlation in Jewish patients suffering from Familial Mediterranean Fever (FMF). Eur J Hum Genet **6**:95–97, 1998.

11. Tidow N, Chen X, Muller C, Kawano S, Gombart AF, Fischel-Ghodsian N, Koeffler HP. Hematopoietic-specific expression of MEFV, the gene mutated in Familial Mediterranean Fever, and subcellular localization of its corresponding protein, pyrin. Blood **95:**1451–1455, 2000.
12. Fields S, Song OK. A novel genetic system to detect protein-protein interactions. Nature **340:**245–246, 1989.
13. Walter DM, Paul KS, Waters MG. Purification and characterization of a novel 13S hetero-oligomeric protein complex that stimulates *in vitro* Golgi transport. J Biol Chem **45:**29565–29576, 1998.
14. Gietz D, St. Jean A, Woods RA, Schiestl RH. Improved method for high efficiency transformation of intact yeast cells. Nucl Acids Res **20:**1425, 1992.
15. Schneider S, Buchert M, Hovens CM. An *in vitro* assay of β-galactosidase from yeast. Biotechniques **20:**960–962, 1996.
16. Altschul SF, Madden TL, Schäffer AA, Zhang J, Zhang Z, Miller W, Lipman DJ. Gapped BLAST, PSI-BLAST: A new generation of protein database search programs. Nucl Acids Res **25:**3389–3402, 1997.
17. Chalfie M, Tu Y, Euskirchen G, Ward WW, Prasher DC. Green fluorescent protein as a marker for gene expression. Science **263:**802–805, 1994.
18. Bouffard GG, Idol JI, Brade VV, Iyer LM, Cunningham AF, Weintraub LA, Touchman JW, Nohr-Tidwell RM, Peluso DC, Fulton RS, Ueltzen MS, Weissenbach J, Magness CL, Green ED. A physical map of human chromosome 7: An integrated YAC contig map with average STS spacing of 79 kb. Genome Res **7:**673–692, 1997.
19. Gattung S. The sequence of *Homo sapiens* BAC clone GR020D02. Direct submission to GenBank (Accession AC002381), 1997.
20. Gattung S, Andrews S, Scronce D. The sequence of *Homo sapiens* PAC clone DJ067311. Direct submission to GenBank (Accession AC004855), 1998.
21. Cordes M. The sequence of *Homo sapiens* BAC clone RG363E19. Direct submission to GenBank (Accession AC004429), 1998.
22. Le Beau MM, Espinosa R, Davis EM, Eisenbart JD, Larson RA, Green ED. Cytogenetic and molecular delineation of a region of chromosome 7 commonly deleted in malignant myeloid diseases. Blood **88:**1930–1935, 1996.
23. Ruutu P, Ruutu T, Vuopio P, Kosunen TU, de la Chapelle A. Defective chemotaxis in monosomy 7. Nature **265:**146–147, 1977.
24. Fields S, Sternglanz R. The two-hybrid system: An assay for protein-protein interactions. Trends Genet **10:**286–292, 1994.
25. Luban J, Goff SP. The yeast two-hybrid system for studying protein-protein interactions. Current Biol **6:**59–64, 1995.
26. Fritzler MJ, Etherington J, Sokoluk C, Kinsella TD, Valencia DW. Antibodies from patients with autoimmune disease react with a cytoplasmic antigen in the Golgi apparatus. J Immunol **132:**2904–2908, 1984.
27. Rossie KM, Piesco NP, Charley MR, Oddis CV, Steen VD, Fratto J, Deng JS. A monoclonal antibody recognizing Golgi apparatus produced using affinity-purified material from a patient with connective tissue disease. Scand J Rheumatol **21:**109–115, 1992.
28. Blaschek MA, Pennec YL, Simitzis AM, Le Goff P, Lamour A, Kerdraon G, Jouquan J, Youinou P. Anti-Golgi complex autoantibodies in patients with primary Sjogren's syndrome. Scand J Rheumatol **17:**291–296, 1988.